

Phase Equilibria in Ionic Liquid–Aromatic Compound Mixtures, Including Benzene Fluorination Effects

Marijana Blesic,[†] José N. Canongia Lopes,^{*,‡,§} Agílio A. H. Pádua,[§] Karina Shimizu,^{†,‡} Margarida F. Costa Gomes,[§] and Luís Paulo N. Rebelo^{*,†}

Instituto de Tecnologia Química e Biológica, ITQB 2, Universidade Nova de Lisboa, Apartado 127, 2780-901 Oeiras, Portugal, Centro de Química Estrutural, Instituto Superior Técnico, 1049-001 Lisboa, Portugal, and Laboratoire Thermodynamique et Interactions Moléculaires, CNRS/Université Blaise Pascal, Clermont-Ferrand, France

Received: March 11, 2009; Revised Manuscript Received: April 13, 2009

This work extends the scope of previous studies on the phase behavior of mixtures of ionic liquids with benzenes or its derivatives by determining the solid–liquid and liquid–liquid phase diagrams of mixtures containing an ionic liquid and a fluorinated benzene. The systems studied include 1-ethyl-3-methylimidazolium bis(trifluoromethanesulfonyl)imide plus hexafluorobenzene or 1,3,5-trifluorobenzene and 1-ethyl-3-methylimidazolium triflate or *N*-ethyl-*N*-methylpyrrolidinium bis(trifluoromethanesulfonyl)imide plus benzene. The phase diagrams exhibit different kinds of solid–liquid behavior: the (usual) occurrence of eutectic points; the (not-so-usual) presence of congruent melting points and the corresponding formation of inclusion crystals; or the observation of different ionic liquid crystalline phases (polymorphism). These different types of behavior can be controlled by temperature annealing during crystallization or by the nature of the aromatic compound and can be interpreted, at a molecular level, taking into account the structure of the crystals or liquid mixtures, together with the unique characteristics of ionic liquids, namely the dual nature of their interactions with aromatic compounds.

Introduction

Binary mixtures of ionic liquids with benzene or its derivatives exhibit unusual phase diagrams.^{1,2} In some cases it is possible to dissolve up to 80% mole fraction of benzene in a given ionic liquid but effectively no ionic liquid in pure benzene. The liquid–liquid immiscibility windows are then markedly skewed toward aromatic-rich compositions,³ a fact which is shared primarily by binary systems in which a large difference between the molar volumes of the components exists.⁴ This behavior has been proven useful for different types of applications,^{5,6} from improved separation techniques (aromatic–aliphatic partition using ionic liquids,⁷ solute extraction in biphasic aromatic–ionic liquid systems⁸) to new reaction or catalytic schemes involving ionic liquid solvents (for example, polymerization,⁹ hydrogenation,¹⁰ or Friedel–Crafts alkylation¹¹).

From a more fundamental, molecular-oriented perspective, these systems were analyzed by Holbrey et al.,¹² Lynden-Bell et al.,¹³ Deetlefs et al.,¹⁴ and Lachwa et al.,² who discussed the possibility of liquid clathrate formation in ionic liquid–aromatic systems. In the first three works it was possible to isolate and characterize by X-ray diffraction a 2:1 (ionic liquid):(benzene) inclusion crystal, and elucidate by neutron diffraction and molecular dynamics studies the structure of the liquid mixtures. Lachwa et al.^{1,2} have shown how the fluid-phase behavior (liquid–liquid immiscibility window) could be fine-tuned by the nature of the ionic liquid or the molecular component, and how the existence of liquid clathrates could be further substanti-

ated from the detection and characterization of a new 1:1 benzene:ionic liquid inclusion crystal exhibiting a congruent melting point above the temperature of both pure substances. Recently, Shiflett and Yokozeki¹⁵ extended the scope of the work involving ionic liquids and aromatic compounds by analyzing the liquid–liquid equilibria in binary mixtures containing fluorinated benzenes and one ionic liquid.

In this work, the line of investigation pursued by some of the studies mentioned in the previous paragraph was continued by determining the solid–liquid and liquid–liquid phase diagrams of benzene plus ionic liquid mixtures, where the nature of the ionic liquid and the nature of the molecular solvent were changed in a deliberate and systematic way in order to elucidate from a molecular point of view the peculiar behavior of this type of system. Taking as the starting point the 1-ethyl-3-methylimidazolium bis(trifluoromethanesulfonyl)imide ionic liquid plus benzene mixtures ([C₂mim][NTf₂] + C₆H₆),^{2,15} it was decided to study two mixtures of that ionic liquid with hexafluorobenzene or 1,3,5-trifluorobenzene ([C₂mim][NTf₂] + C₆F₆ and [C₂mim][NTf₂] + C₆H₃F₃). The phase behavior of these mixtures was characterized not only in terms of the liquid–liquid immiscibility, as in the study recently reported by Shiflett,¹⁵ but also in terms of the solid–liquid equilibria. The main objective was to check the effect of changing the aromatic character and charge distribution of the benzene derivative on the phase behavior of the mixtures. This set of results was complemented by the determination of the phase diagram of the system [C₂mim][NTf₂] plus cyclohexane ([C₂mim][NTf₂] + c-C₆H₁₂), where the aromatic nature of the molecular component of the system is completely absent. In order to check the influence of replacing a cation containing an aromatic ring (imidazolium) by another with a nonaromatic cation (pyrrolidinium), the system [C₁C₂pyrr][NTf₂] + C₆H₆ was

* Corresponding authors. E-mail: luis.rebelo@itqb.unl.pt (L.P.N.R.); jnlopes@ist.utl.pt (J.N.C.L.).

[†] Universidade Nova de Lisboa.

[‡] Instituto Superior Técnico.

[§] CNRS/Université Blaise Pascal.

also studied. Finally, the effect on the phase behavior of changing the anion of the ionic liquid was studied by comparing the behavior of mixtures containing the bis(trifluoromethanesulfonyl)imide anion with others including the smaller trifluoromethanesulfonate anion as in the $[\text{C}_2\text{mim}][\text{OTf}] + \text{C}_6\text{H}_6$ system. In this case any changes in the phase diagram reflect the influence of the benzene–anion interactions (including the loss of flexibility of the anion when changing from $[\text{NTf}_2]^-$ to $[\text{OTf}]^-$).

Experimental Section

Materials. 1-Ethyl-3-methylimidazolium bis(trifluoromethanesulfonyl)imide, $[\text{C}_2\text{mim}][\text{NTf}_2]$, was purchased from Solvent Innovation with 99% purity. 1-Ethyl-3-methylimidazolium trifluoromethanesulfonate, $[\text{C}_2\text{mim}][\text{OTf}]$, and 1-ethyl-3-methylpyrrolidinium bis(trifluoromethanesulfonyl)imide, $[\text{C}_2\text{C}_1\text{pyrr}][\text{NTf}_2]$, were purchased from Iolitec, both with 99% purity. Vacuum (0.1 Pa) and moderate temperature (70 °C) conditions were always applied to all ionic liquid samples for several days prior to their use, in order to reduce their water and other volatile substances content. The fluorinated molecular solvents, hexafluorobenzene and 1,3,5-trifluorobenzene, were purchased from Apollo with 99% purity and were used without further purification. Benzene and cyclohexane (Aldrich, 99.5%) were dried with 3 Å molecular sieves prior to the measurements.

Liquid–Liquid Equilibrium (LLE) Measurements. All cloud-point determinations on the temperature–composition phase diagrams corresponding to liquid–liquid equilibria at a nominal pressure of 0.1 MPa were performed using a dynamic method with visual detection of the solution turbidity. For this purpose, Pyrex glass view cells with magnetic stirring were used. Samples were gravimetrically prepared directly inside the cells using an analytical high-precision balance (± 0.01 mg). The cells were then immersed in a thermostatic bath. Providing continuous stirring, the solutions were cooled or heated, usually in two or three consecutive runs with the two last runs being carried out very slowly (the rate of temperature change near the cloud point was not greater than $5 \text{ K} \cdot \text{h}^{-1}$). Starting from the homogeneous region, the temperature at which the first sign of turbidity appeared upon cooling was taken as the temperature of the liquid–liquid phase transition.

Solid–Liquid Equilibrium (SLE). The solid–liquid equilibrium temperatures at 0.1 MPa nominal pressure were determined using the following methodology: mixtures of the ionic liquid plus the molecular component were placed in a Pyrex glass cell. The cell was then inserted in a thermostatic water or ethanol bath and cooled by adding ice or liquid nitrogen, respectively. After solidification, the samples were heated very slowly (less than $2 \text{ K} \cdot \text{h}^{-1}$ near the equilibrium temperature) with continuous stirring inside the cell during the melting process. The temperature at which the last crystal disappeared was taken as the temperature of the solid–liquid equilibrium.

Both the crystal disappearance temperatures and the cloud-point temperatures were measured using a four-wire platinum resistance thermometer coupled to a Yokogawa 7561 multimeter. The thermometer was calibrated against high accuracy mercury thermometers (0.01 K precision). The overall uncertainty of the transition temperature measurements, resulting from the visual observation of the turbidity (LLE) or the disappearance of the last crystals (SLE), estimated to be ± 1 K, is obviously greater than the instrumental error.

Results and Discussion

The T – x phase diagrams of the systems $[\text{C}_2\text{mim}][\text{NTf}_2] + \text{C}_6\text{F}_6$, $[\text{C}_2\text{mim}][\text{NTf}_2] + 1,3,5\text{-C}_6\text{H}_3\text{F}_3$, and $[\text{C}_2\text{mim}][\text{NTf}_2] + \text{c-C}_6\text{H}_{12}$ are presented in Figure 1. The data presented in Figure 1a–c are also given in Table S1 of the Supporting Information. For comparison purposes Figure 1d overlaps the most important phase transition boundaries for each system along with those of the previously studied $[\text{C}_2\text{mim}][\text{NTf}_2] + \text{C}_6\text{H}_6$ system.^{1,2}

Some obvious conclusions can be taken directly from the analysis of Figure 1: (a) The solubility of the ionic liquid in any of the molecular solvents is always almost null. In all cases the L + L regions start just at the pure molecular solvent line; cf. upper left sides of the phase diagrams. (b) Differences are much more evident at the other end of the L + L immiscibility windows; cf. vertical lines along the top of Figure 1d. The solubility of the aliphatic compound is much smaller ($x_{\text{mol}}(\text{c-C}_6\text{H}_{12}) < 0.10$) than that of the aromatic solvents. The latter exhibit solubilities corresponding to mole fractions of $x_{\text{mol}}(\text{C}_6\text{H}_6) = 0.78$, $x_{\text{mol}}(\text{C}_6\text{F}_6) = 0.66$, and $x_{\text{mol}}(\text{C}_6\text{F}_3\text{H}_3) = 0.55$, to be compared with the results of Shiflett and Yokozeki¹⁵ of 0.76, 0.66, and 0.50, respectively. (c) Benzene is the most soluble of the aromatic compounds in terms of molar fraction, but if the molar volumes and densities of each component are taken into account and solubility is expressed as volumetric or mass fractions, then the solubility differences change to $x_{\text{vol}}(\text{C}_6\text{H}_6) = 0.55$, $x_{\text{vol}}(\text{C}_6\text{F}_6) = 0.47$, and $x_{\text{vol}}(1,3,5\text{-C}_6\text{H}_3\text{F}_3) = 0.33$, or $x_{\text{mass}}(\text{C}_6\text{H}_6) = 0.41$, $x_{\text{mass}}(\text{C}_6\text{F}_6) = 0.48$, and $x_{\text{mass}}(1,3,5\text{-C}_6\text{H}_3\text{F}_3) = 0.29$, with the solubilities of C_6H_6 and C_6F_6 lying closer to each other than that of 1,3,5- $\text{C}_6\text{H}_3\text{F}_3$. (d) The most important difference between the phase diagrams of the systems containing the fluorinated benzene molecules and the one corresponding to normal benzene is the absence of any congruent melting inclusion compound in the former systems. On the other hand, multiple polymorphic forms of $[\text{C}_2\text{mim}][\text{NTf}_2]$ were observed in the fluorinated benzene systems (not shown in Figure 1d but depicted in Figure 1a,b), which corroborates the findings of Paulechka et al.¹⁶ In conclusion, the substituted benzenes are also capable of permeating the polar network of the ionic liquid,¹⁷ but are not able to interact so efficiently as benzene (or at least in a such a well-defined stereochemical way) in order to form inclusion compounds.² This is probably due to the lack or deficiency of hydrogen atoms at the equatorial positions of the aromatic ring, responsible for the connections with the oxygen atoms of the $[\text{NTf}_2]^-$ anion.²

The structures of $[\text{C}_2\text{mim}][\text{NTf}_2] +$ fluorinated benzene binary mixtures were further analyzed using molecular simulation. Molecular dynamics runs at 298 K were performed using the DL_POLY package.¹⁸ An all-atom force field based on a version of the AMBER/OPLS-AA framework extended to encompass ionic liquids of the $[\text{C}_n\text{mim}][\text{NTf}_2]$ family^{19–21} was used to describe the ionic liquid component. An OPLS-AA parametrization was used for benzene, perfluorobenzene, and 1,3,5- $\text{C}_6\text{H}_3\text{F}_3$.²² The binary mixtures were modeled in boxes with 384 ions and 64 molecular species, cutoff distances of 2.0 nm, and the usual Ewald summation technique to account for long-range interactions. More details on this type of simulation, involving finite concentrations of solute molecules in ionic liquids, can be found elsewhere.²³ The simulation data were obtained in production runs of 600 ps that started only after an equilibration period of 1.2 ns. The MD results are summarized in Figure 2, where spatial distribution functions, showing the position of the cations and anions of the ionic liquid around the benzene molecules, are presented.

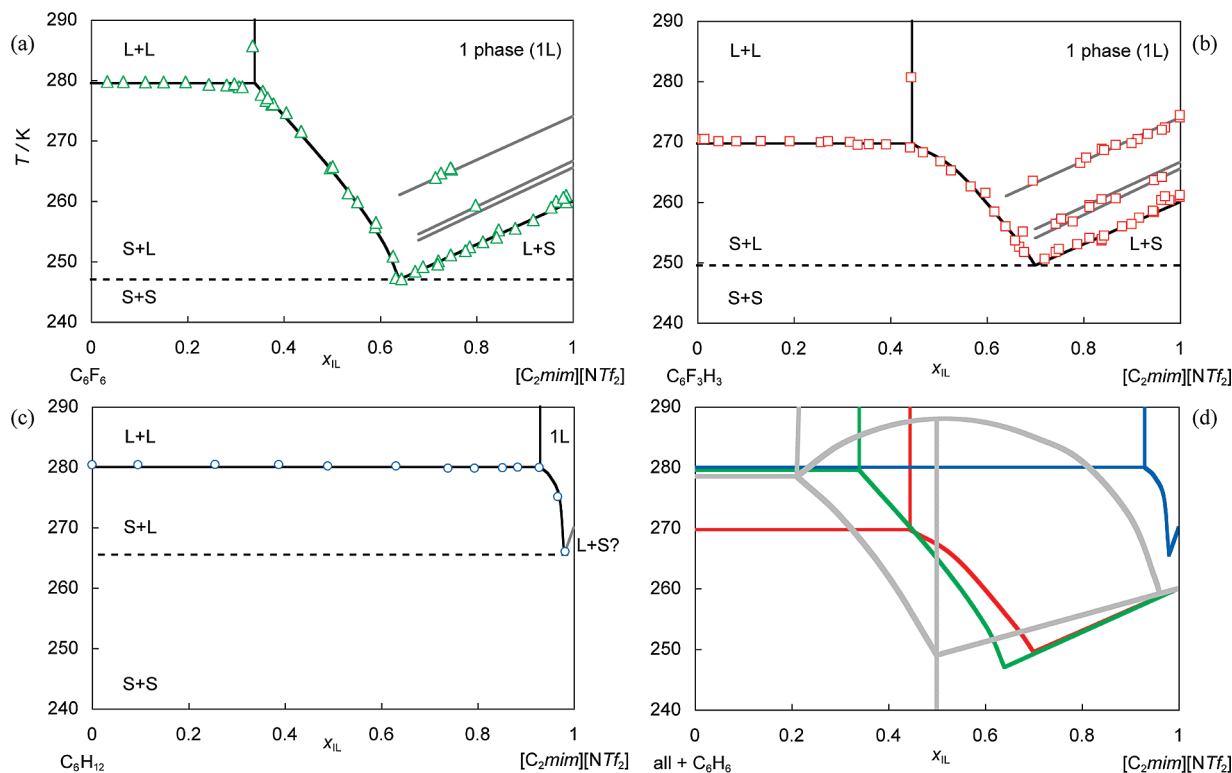


Figure 1. T - x phase diagrams of systems containing [C₂mim][NTf₂] mixed with (a) C₆F₆, (b) 1,3,5-C₆H₃F₃, or (c) c-C₆H₁₂. Part d overlaps the different diagrams (keeping the same color convention used in (a)–(c) along with the schematic representation, in gray, of the phase diagram of [C₂mim][NTf₂] + C₆H₆.^{1,2} In (a) and (b) the gray lines represent the precipitation of different polymorphs of [C₂mim][NTf₂] during the cooling of the mixtures and are given just as an aid to the eye. The dashed lines are three-phase lines corresponding to the eutectic temperature of each mixture.

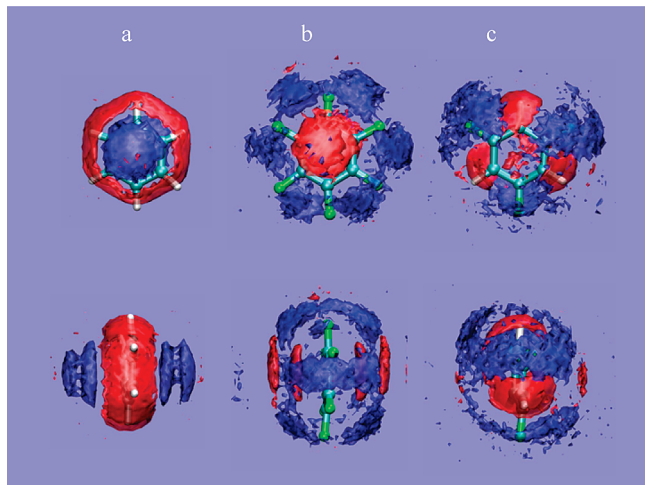


Figure 2. Spatial distribution functions of systems containing [C₂mim][NTf₂] mixed with (a) C₆H₆, (b) C₆F₆, and (c) 1,3,5-C₆H₃F₃. The images show the distribution of the oxygen (O) atoms of the anion (in red) and the C2 carbon of the imidazolium ring (in blue) around a central aromatic molecule. The isosurfaces depicted correspond to densities of 1.8 for O and 2.5 for C2 in (a), 1.8 for O and 2.2 for C2 in (b), and 1.9 for O and 2.2 for C2 in (c), relative to the average densities of those atoms in the mixtures.

Similar simulations, involving an ionic liquid plus benzene or hexafluorobenzene mixtures, had been previously carried out by Lynden-Bell and co-workers.¹³ The novelties of the present work include the study of mixtures containing trifluorinated benzene and the modeling of the same ionic liquid studied experimentally (both in this work and in ref 2): [C₂mim][NTf₂]. In the case of benzene, X-ray data (solid phase) and simulations (liquid phase) show similar structural arrangements around the

aromatic molecules (Figure 3 from ref 2 and Figure 2 of this work): the anions of the ionic liquid can be found around the equatorial region of the aromatic plane, whereas the cations occupy the polar regions above and below that plane (cation- π interactions). The opposite situation (cations at the equator, anions at the poles) is found for hexafluorobenzene. This means that the charged regions of the ionic liquid will position themselves according to the molecular quadrupole moments of the benzene and hexafluorobenzene molecules. These quadrupoles lie normal to the aromatic plane of the molecules and are negative in the case of benzene (around $-30 \times 10^{-40} \text{ C} \cdot \text{m}^2$), a consequence of positive partial charges at the equator of the molecule, and positive in the case of hexafluorobenzene (around $+30 \times 10^{-40} \text{ C} \cdot \text{m}^2$), denoting the inverse effect.

In addition, in the case of the [C₂mim][NTf₂] + C₆H₆ system, X-ray diffraction data² have shown the existence of hydrogen-bond-like interactions between the oxygen atoms of the bistriflamide anions placed at the equator of the benzene molecules and the hydrogen atoms of the latter molecule. In hexafluorobenzene, where all the hydrogen atoms are replaced by fluorine atoms, this type of interaction is replaced by hydrogen bond interactions between F and the acidic hydrogen atoms of the cations. However, since the latter interaction is probably less intense than the former (the access to the hydrogen atoms of the cation is partially hindered by the alkyl side chains of the cation, therefore the “ambident” character of the double pair of oxygen atoms of bistriflamide is no longer participating in hydrogen bonding), it can help explain that no inclusion crystal was found in the [C₂mim][NTf₂] + C₆F₆ system.

In the system containing trifluorinated benzene, the almost vanishing molecular quadrupole moment ($+3.4 \times 10^{-40} \text{ C} \cdot \text{m}^2$) means that the arrangement of the ions around it is much weaker

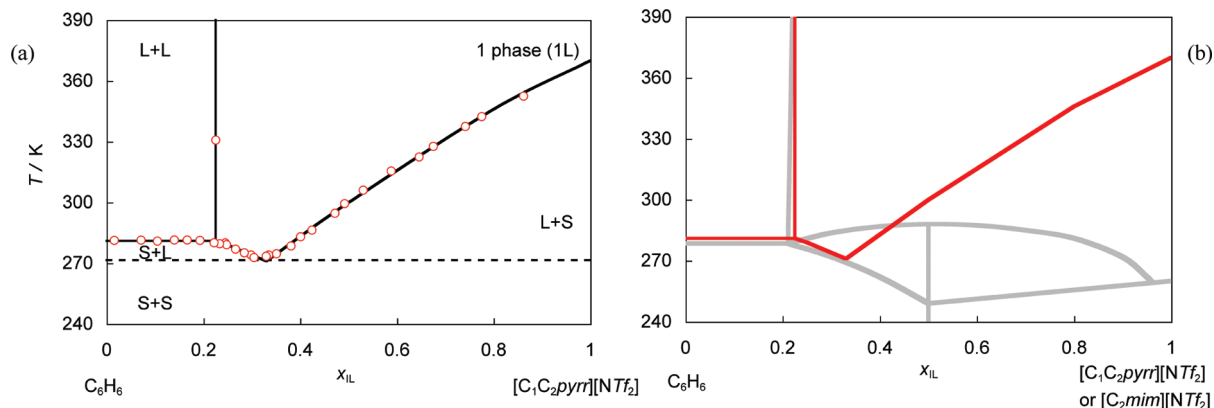


Figure 3. T - x phase diagrams of systems containing $[C_2C_1pyrr][NTf_2]$ mixed with C_6H_6 . Part b overlaps the diagram of (a) with the schematic representation in gray of the phase diagram of $[C_2mim][NTf_2] + C_6H_6$.² The dashed lines are three-phase lines corresponding to the eutectic temperature of each mixture.

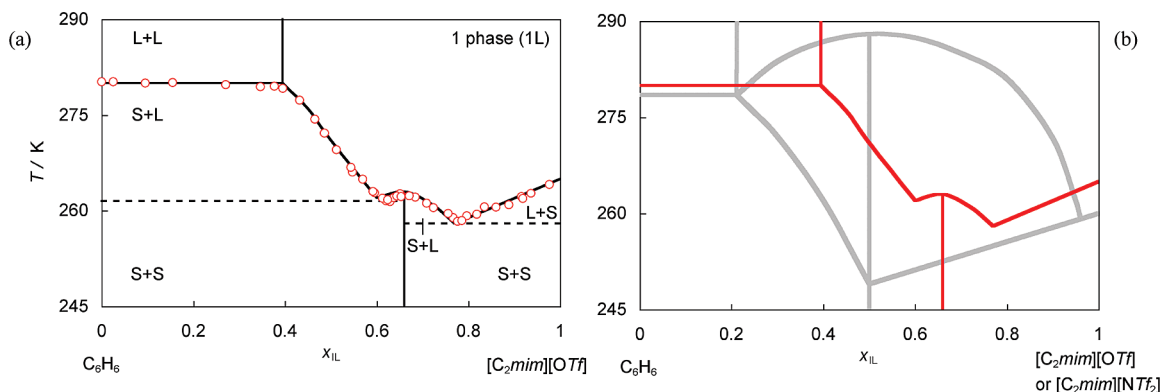


Figure 4. T - x phase diagrams of systems containing $[C_2mim][OTf]$ mixed with C_6H_6 . Part b overlaps the diagram of (a) with the schematic representation in gray of the phase diagram of $[C_2mim][NTf_2] + C_6H_6$.² The vertical lines correspond to congruent melting compounds. The dashed lines are three-phase lines corresponding to the eutectic temperature of each mixture.

(Figure 2c). The lower solubility of 1,3,5- $C_6F_3H_3$ when compared to those of C_6H_6 and C_6F_6 can be explained by weaker multipole-ion interactions, although the specific interactions between the hydrogen atoms and the anions and the fluorine atoms and the cations are still (partially) there and might explain the relatively enhanced solubility of $C_6F_3H_3$ when compared to cyclohexane.

The phase diagram of the system $[C_2C_1pyrr][NTf_2] + C_6H_6$ is shown in Figure 3. The data are also presented in Table S1 of the Supporting Information. In this case, the aromatic nature of the cation constituting the ionic liquid is absent as the imidazolium is replaced by a pyrrolidinium ring. The liquid-liquid immiscibility region (the circle in the upper left corner of Figure 3a) is almost identical with that observed in the case of the $[C_2mim][NTf_2] + C_6H_6$ system (Figure 3b). In previous studies concerning (ionic liquid + aromatic) systems, the existence and nature of π - π interactions between the aromatic rings of the cations (in most cases imidazolium- or pyridinium-based) and the rings of the aromatic molecules have allowed an explanation of the behavior found. In some cases the existence of those interactions was suggested to be directly linked to the performance of ionic liquid solvents as catalytic agents for reactions involving aromatic molecules.^{6,10,11} Although this link is real, it does not necessarily imply that aromatic molecules must be more soluble in ionic liquids that have aromatic rings in their structure as compared to ionic liquids that do not have those rings: the pyrrolidinium cation used in this study is an obvious example. In other words, whenever chemical reactions that involve aromatic molecules occur, the existence of aromatic rings in the ionic liquid can play an important part in the process;

however, that factor does not play a significant role in the determination of liquid-liquid immiscibility of aromatic compounds in ionic liquids.

Even if the L-L immiscibility is unaffected by the absence of aromatic rings in the cations, the same is not true as regards the formation of inclusion compounds; as seen in the previous $[C_2mim][NTf_2]$ plus fluorinated benzene systems, a change in the aromatic character of the molecular component precludes the formation of the inclusion compounds similar to $[C_2mim][NTf_2] \cdot C_6H_6$. No inclusion compound was found in the case of $[C_2C_1pyrr][NTf_2] + C_6H_6$, although it is difficult to establish a direct link with the absence of an aromatic ring in the cation. In fact, the melting point of $[C_2C_1pyrr][NTf_2]$ is much higher than that of $[C_2mim][NTf_2]$, which means that the crystalline forms of the former ionic liquid are much more stable than those of the latter. The driving forces toward the formation of inclusion crystals are not present in the system $[C_2C_1pyrr][NTf_2] + C_6H_6$, either due to the lack of an aromatic ring in the cations (and the absence of stabilizing π - π interactions between benzene and the cations), or due to the much more stable (pure) $[C_2C_1pyrr][NTf_2]$ crystals. This last argument can be qualitatively inferred from Figure 3b, where it can be seen that the $[C_2mim][NTf_2] \cdot C_6H_6$ inclusion compound is "hidden" below the precipitation line of $[C_2C_1pyrr][NTf_2]$ (red and gray lines on the right-hand side of Figure 3b). It must be noted that a 3:1 inclusion compound was reported for the mixture $[C_2mim][NTf_2]$ plus tetrahydrofuran (THF),²⁴ lending some support to the view that π - π interactions between the ionic liquid and the solute are not a necessary (or sufficient) condition to the occurrence of inclusion compounds.

Figure 4 shows the phase diagram of the system $[\text{C}_2\text{mim}][\text{OTf}] + \text{C}_6\text{H}_6$. The experimental T – x data points used to build the phase diagram are compiled in Table S1 of the Supporting Information. In this case the aromatic molecular components of the system were left intact, and only the flexible and large $[\text{NTf}_2]^-$ ion was replaced by the more rigid and smaller triflate anion, whose oxygen atoms are also capable of strong interactions with the aromatic hydrogens of benzene. This means that the changes in the interaction patterns between the ionic and molecular components of the mixture are quite subtle when compared to the reference $[\text{C}_2\text{mim}][\text{NTf}_2] + \text{C}_6\text{H}_6$ system as reflected in the phase diagram depicted in Figure 4a that exhibits a 2:1 $[\text{C}_2\text{mim}][\text{OTf}] \cdot \text{C}_6\text{H}_6$ inclusion crystal. However, when comparing the two inclusion crystals in Figure 4b, two conclusions are obvious: they do not occur with the same stoichiometry and their stabilities are quite different. The melting point temperature of the 2:1 inclusion crystal is lower than those of the corresponding pure components. Also, the solubility of the benzene molecules in the $[\text{C}_2\text{mim}][\text{OTf}] + \text{C}_6\text{H}_6$ system, $x(\text{C}_6\text{H}_6) = 0.61$, is depressed relative to the $[\text{C}_2\text{mim}][\text{NTf}_2] + \text{C}_6\text{H}_6$ system, $x(\text{C}_6\text{H}_6) = 0.78$. However, one must keep in mind that in terms of volumetric or mass fractions this is not so pronounced: $x_{\text{vol}}(\text{C}_6\text{H}_6) = 0.42$ and 0.55 , or $x_{\text{mass}}(\text{C}_6\text{H}_6) = 0.32$ and 0.41 , for the $[\text{C}_2\text{mim}][\text{OTf}] + \text{C}_6\text{H}_6$ and $[\text{C}_2\text{mim}][\text{NTf}_2] + \text{C}_6\text{H}_6$ systems, respectively. The stoichiometry is explained by the size of the molecular compounds: more ions are needed to surround one benzene molecule in order to form a stable crystalline structure. In fact, a similar situation has already been reported in the case of the previously studied 2:1 $[\text{C}_1\text{mim}][\text{PF}_6] \cdot \text{C}_6\text{H}_6$ inclusion crystal,¹² where the smaller size of the ions (specially the anion) also accounted for the different ionic-to-molecular component ratio in the crystal.

The relative stability of the inclusion crystals is more difficult to interpret, but it can be related to the flexibility and ambident character of the $[\text{NTf}_2]^-$ anion (stronger, better oriented benzene–anion interactions),² or simply to the different stoichiometry (more benzene–anion interactions) of the inclusion crystals. Unfortunately, it was not possible to isolate and analyze by X-ray diffraction a single crystal of the $[\text{C}_2\text{mim}][\text{OTf}]_2 \cdot \text{C}_6\text{H}_6$ inclusion compound, which means that no further conclusions are possible at this stage.

Conclusions

Previous studies by the authors of the present work emphasize the so-called doubly dual nature of ionic liquids.¹⁷ On the one hand, this unique class of compounds are now regarded as nanosegregated liquids constituted by a polar network permeated by nonpolar domains (formed by the noncharged parts of the large, organic ions of many ionic liquids). This means that there will be a competition between the interactions of a given solute with those two regions (polar versus nonpolar). On the other hand, one can never forget that the polar network is composed of two types of ions with opposite charges and very different outlooks in terms of interaction (cations versus anions). The systems studied herein stress the second aspect of the dual nature of ionic liquids by considering different ionic liquids (all with ions with small noncharged parts and therefore negligible influence of nonpolar domains) mixed with different solutes. In the case of fluorinated benzenes the change in the sign of the molecular quadrupole moment of the solutes (or its absence) allowed us to highlight in a remarkable way how this dual nature of ionic liquids can be used to tailor the structure (and behavior) of ionic liquids when mixed with various solutes. This line of research will be pursued in a future publication, where the

relative solubility of benzene plus its 12 fluorinated derivatives (experimentally determined by Shiflett and Yokozeki¹⁵) will be rationalized in terms of the relations between the dual nature of ionic liquids (competing interactions to cations and anions), the multipolar nature of the aromatic solutes, and the resulting structural characteristics of the mixtures.

Acknowledgment. This work was supported by the Fundação para a Ciência e Tecnologia (FC&T), Portugal (POCI/QUI/57716/2004 and PTDC/CTM/73850/2006). M.B. and K.S. acknowledge Grants SFRH/BD/13763/2003 and SFRH/BPD/38339/2007, respectively. A.A.H.P. and M.F.C.G. would like to recognize the support of the “Prof. António Xavier Excellence Award” by the Oeiras City Council.

Supporting Information Available: Table S1, experimental LLE and SLE data. This material is available free of charge via the Internet at <http://pubs.acs.org>.

References and Notes

- (1) Lachwa, J.; Szydłowski, J.; Makowska, A.; Seddon, K. R.; Esperança, J. M. S. S.; Guedes, H. J. R.; Rebelo, L. P. N. Changing from an unusual high-temperature demixing to a UCST-type in mixtures of 1-alkyl-3-methylimidazolium bis[(trifluoromethyl)sulfonyl]amide and arenes. *Green Chem.* **2006**, *8*, 262–267.
- (2) Lachwa, J.; Bento, I.; Duarte, M. T.; Lopes, J. N. C.; Rebelo, L. P. N. Condensed phase behaviour of ionic liquid–benzene mixtures: congruent melting of a $[\text{emim}][\text{NTf}_2] \cdot \text{C}_6\text{H}_6$ inclusion crystal. *Chem. Commun.* **2006**, 2445–2447.
- (3) Rebelo, L. P. N.; Najdanovic-Visak, V.; Gomes de Azevedo, R.; Esperança, J. M. S. S.; Nunes da Ponte, M.; Guedes, H. J. R.; Visak, Z. P.; de Sousa, H. C.; Szydłowski, J.; Canongia Lopes, J. N.; Cordeiro, T. C. Phase behavior and thermodynamic properties of ionic liquids, ionic liquid mixtures and ionic liquid solutions. In *Ionic Liquids IIIA: Fundamentals, Progress, Challenges, and Opportunities, Properties and Structure*; ACS Symposium Series 901; Rogers, R. D., Seddon, K. R., Eds.; American Chemical Society: Washington, DC, 2005; pp 270–291.
- (4) (a) Rebelo, L. P. N. A simple g^E -model for generating all basic types of binary liquid–liquid equilibria and their pressure dependence. Thermodynamic constraints at critical loci. *Phys. Chem. Chem. Phys.* **1999**, *1*, 4277–4286. (b) de Sousa, H. C.; Rebelo, L. P. N. A continuous polydisperse thermodynamic algorithm for a modified Flory–Huggins model: The (polystyrene + nitroethane) example. *J. Polym. Sci., B: Polym. Phys.* **2000**, *38*, 632–651.
- (5) Blanchard, L. A.; Brennecke, J. F. Recovery of organic products from ionic liquids using supercritical carbon dioxide. *Ind. Eng. Chem. Res.* **2001**, *40*, 287–292.
- (6) Surette, J. K. D.; Green, L.; Singer, R. D. 1-Ethyl-3-methylimidazolium halogenoaluminate melts as reaction media for the Friedel–Crafts acylation of ferrocene. *Chem. Commun.* **1996**, 2753–2754.
- (7) Kato, R.; Krummen, M.; Gmehling, J. Measurement and correlation of vapor–liquid equilibria and excess enthalpies of binary systems containing ionic liquids and hydrocarbons. *Fluid. Phase Equilib.* **2004**, *224*, 47–54.
- (8) Huddleston, J. G.; Visser, A. E.; Reichert, W. M.; Willauer, H. D.; Broker, G. A.; Rogers, R. D. Characterization and comparison of hydrophilic and hydrophobic room temperature ionic liquids incorporating the imidazolium cation. *Green Chem.* **2001**, *3*, 156–164.
- (9) Csihony, S.; Fischmeister, C.; Bruneau, C.; Horvath, I. T.; Dixneuf, P. H. First ring-opening metathesis polymerization in an ionic liquid. Efficient recycling of a catalyst generated from a cationic ruthenium allenylidene complex. *New J. Chem.* **2002**, *26*, 1667–1670.
- (10) Boxwell, C. J.; Dyson, P. J.; Ellis, D. J.; Welton, T. A highly selective arene hydrogenation catalyst that operates in ionic liquid. *J. Am. Chem. Soc.* **2002**, *124*, 9334–9335.
- (11) DeCastro, C.; Sauvage, E.; Valkenberg, M. H.; Holderich, W. F. Immobilised ionic liquids as Lewis acid catalysts for the alkylation of aromatic compounds with dodecene. *J. Catal.* **2000**, *196*, 86–94.
- (12) Holbrey, J. D.; Reichert, W. M.; Nieuwenhuyzen, M.; Sheppard, O.; Hardacre, C.; Rogers, R. D. Liquid clathrate formation in ionic liquid–aromatic mixtures. *Chem. Commun.* **2003**, 476–477.
- (13) Harper, J. B.; Lynden-Bell, R. M. Macroscopic and microscopic properties of solutions of aromatic compounds in an ionic liquid. *Mol. Phys.* **2004**, *102*, 85–94.
- (14) Deetlefs, M.; Hardacre, C.; Nieuwenhuyzen, M.; Sheppard, O.; Soper, A. K. Structure of ionic liquid–benzene mixtures. *J. Phys. Chem. B* **2005**, *109*, 1593–1598.

- (15) Shiflett, M. B.; Yokozeki, A. Liquid-Liquid Equilibria in Binary Mixtures Containing Fluorinated Benzenes and Ionic Liquid 1-Ethyl-3-methylimidazolium Bis(trifluoromethylsulfonyl)imide. *J. Chem. Eng. Data* **2008**, *53*, 2683–2691.
- (16) Paulechka, Y. U.; Blokhin, A. V.; Kabo, G. J.; Strechan, A. A. Thermodynamic properties and polymorphism of 1-alkyl-3-methylimidazolium bis(triflamides). *J. Chem. Thermodyn.* **2007**, *39*, 866–877.
- (17) (a) Rebelo, L. P. N.; Lopes, J. N. C.; Esperanca, J. M. S. S.; Guedes, H. J. R.; Lachwa, J.; Najdanovic-Visak, V.; Visak, Z. P. Accounting for the unique, doubly dual nature of ionic liquids from a molecular thermodynamic, and modeling standpoint. *Acc. Chem. Res.* **2007**, *40*, 1114–1121. (b) Lopes, J. N. C.; Padua, A. A. H. Nanostructural organization in ionic liquids. *J. Phys. Chem. B* **2006**, *110*, 3330–3335.
- (18) Smith, W.; Forester, T. R. *The DL_POLY package of molecular simulation routines*, version 2.13; The Council for the Central Laboratory of Research Councils, Daresbury Laboratory: Warrington, U.K., 1999.
- (19) Lopes, J. N. C.; Deschamps, J.; Padua, A. A. H. Modeling ionic liquids using a systematic all-atom force field. *J. Phys. Chem. B* **2004**, *108*, 2038–2047.
- (20) Lopes, J. N. C.; Padua, A. A. H. Molecular force field for ionic liquids composed of triflate or bistriflylimide anions. *J. Phys. Chem. B* **2004**, *108*, 16893–16898.
- (21) Padua, A. A. H.; Gomes, M. F. C.; Lopes, J. N. C. Molecular solutes in ionic liquids: A structural, perspective. *Acc. Chem. Res.* **2007**, *40*, 1087–1096.
- (22) Watkins, E. K.; Jorgensen, W. L. Perfluoroalkanes: Conformational analysis and liquid-state properties from ab initio and Monte Carlo calculations. *J. Phys. Chem. A* **2001**, *105*, 4118–4125.
- (23) Lopes, J. N. C.; Gomes, M. F. C.; Padua, A. A. H. Nonpolar, polar, and associating solutes in ionic liquids. *J. Phys. Chem. B* **2006**, *110*, 16816–16818.
- (24) Domanska, U.; Marciniak, A.; Królikowski, M. Phase equilibria and modeling of ammonium ionic liquid, C2NTf2, solutions. *J. Phys. Chem. B* **2008**, *112*, 1218–1225.

JP902178G